Supplementary Information: Membrane permeability to water measured by microfluidic trapping of giant vesicles

Tripta Bhatia*, Tom Robinson, Rumiana Dimova*

Received Xth XXXXXXXXXX 20XX, Accepted Xth XXXXXXXXX 20XX
First published on the web Xth XXXXXXXXXX 200X
DOI: 10.1039/b000000x

1 Microfluidic device

The microfluidic devices that are used in the experiments consist of 108 trapping chambers shown in Fig. S1. The microfluidic chips were fabricated from polydimethylsiloxane (PDMS) and consisted of a two-layer design, the fabrication of which has been described previously.[1] The inlet (in) for introducing the sample such as GUVs, is shown as well as the outlet (out). r_1, r_2, r_3, r_4 show the width of the channels at respective positions where $r_1 = 50\ \mu$m, $r_2 = 950\ \mu$m, $r_3 = 50\ \mu$m, $r_4 = 20\ \mu$m. The green circles are showing the inlets of the 6 pressure channels. A red circle showing a single trap is investigated further in Fig. S2.

Figure S2 shows 3D schematic of a single chamber with a GUV trap. Each trapping chamber consist of a series of 15 micron-sized PDMS posts of individual size $\sim$ ($20\ \mu$m $\times$ $20\ \mu$m $\times$ $20\ \mu$m) separated by $\sim$ $5\ \mu$m that are arranged in a semi-circular or horse-shoe fashion. The vertical height of the chamber and all channels is $\sim 20\ \mu$m. Above each trap there is a circular ring-valve, which is connected to an external pressure control device,[2] the purpose of which is to create a sealed chamber of a defined volume surrounding the trap and GUVs. This is achieved due to the deformable nature of the PDMS membrane separating the upper and lower layers. This volume is fluidically isolated from the rest of channel network and the other chambers. The ring-valves are mechanically actuated up (open) and down (closed), using inlets of 6 pressure channels shown in Fig. S1 (encircled with green color). These permit multiple experiments per chip with each having 18 chambers. Only once the valve is open, the fluid is exchanged, which allows real-time observations of the morphological changes that occur after solution exchange to the final desired concentration.

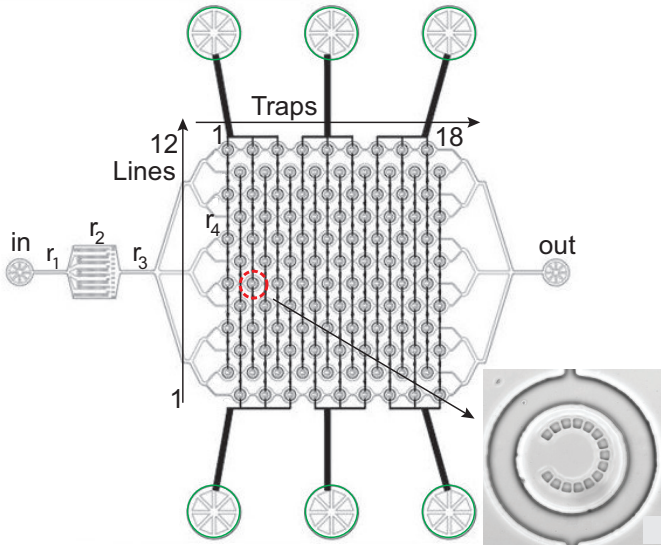

Fig. S1. Schematic of the microfluidic device design used in the experiments and fluid exchange. The device is composed of 108 chambers that are split between 6 separate pressure channels (encircled with green colours). The inlet (in) and outlet (out) are shown. r_1, r_2, r_3, r_4 refer to the radii of the channels at the respective positions. A red circle showing a single net-trap is discussed in Fig.S2.

2 Characterizing the full fluid exchange in the microfluidic chamber

Figure S3a shows a confocal fluorescence image of the xy-plane of a single chamber with trap filled with aqueous solution of the fluorescence dye calcein (green). When the valve is closed (2 bar) as shown in Fig. S3b we have filled the microchannel network with water at high flow rate $Q_{fl} = 25\ \mu$l/min. Figure S3c shows an image of the same chamber after the chip is flushed with calcein-free solution. We find no leakage of calcein from the trapped region if the valve is completely sealed at this applied pressure. Figure S3d

[a] *Theory & Biosystems, Max Planck Institute of Colloids and Interfaces, 14424 Potsdam, Germany.*
* *E-mail: tripta.bhatia@mpikg.mpg.de, dimova@mpikg.mpg.de*

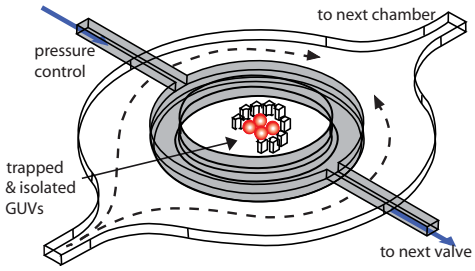

Fig. S2. 3D-schematic of the microfluidic device design used to trap GUVs and controllably exchange solutions. The device is composed of a ring-valve (in gray) connected to a pressure control device. Note that the number of posts and GUVs are more in practice than shown in the schematic.

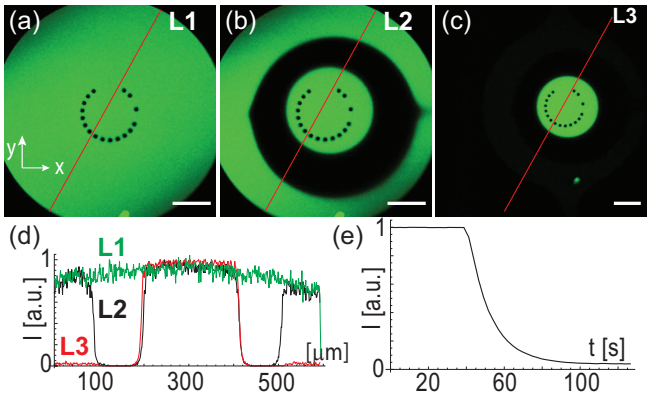

Fig. S3. (a) Confocal fluorescence image of the *xy*-plane of a single chamber with trap filled with aqueous solution of the fluorescence dye calcein (green). The posts (black dots) are arranged in the horse-shoe manner. The vertical height of the chamber is $\sim 20\ \mu$m. (b) The ring-valve (black donut) is closed with $P_{valve} = 2$ bar of pressure. (c) Water without calcein is introduced in the microfluidic device with an external flow-rate of $Q_{fl} = 25\ \mu$l/min that fills the entire microfluidic device but is excluded from the region inside the ring-valve. (d) Line profiles of the fluorescence intensity of calcein for images shown in (b) green curve, (c) black curve and (d) red curve. (e) The plot showing the decrease in the fluorescence intensity of calcein with time at a flow-rate of $Q_{fl} = 0.07\ \mu$l/min after the valve is open for fluid exchange.

shows the fluorescence intensity of calcein along the red lines (L_1, L_2, L_3) shown in Figs. S3a-c.

From the intensity line profiles, it is clear that a single micro-compartment has a uniform radius 300 μm as shown by green line L_1. We estimate the total volume of a single chamber including posts when the ring-valve is open from the intensity line profiles as $V_{\rm ch} \sim \pi(300\ \mu{\rm m})^2 * 20\ \mu{\rm m} \cong 5.65$ nL. The black line L_2 shows the intensity profile when the ring-valve is closed.The red line L_3 shows that intensity line profile when the microchannel network is filled with water giving the area of the trapped region (green region) enclosed by the ring-valve. The volume of the trapped region is approximately 0.5 nL.

Figure S3e shows decrease in fluorescence intensity of calcein when the valve is moved up isotropically with a change of pressure from 2 to 1 bar. In the experiments reported herein, we find that when the valve is partially open at a pressure of about $0.5-0.6$ mbar, then fluid exchange is completed within 40 s. The plot suggests that within 40 s, the inside and outside solutions are equilibrated, in this case aqueous solution of calcein inside the trapped region ($t = 0$) with pure water in the rest of the microchannel network. It is possible to open the valve further and we wait for 12 mins or more to make sure that fluid is fully exchanged.

3 Shape reversibility

In this section, we explore the shape reversibility during multiple solvent exchange. The microfluidic device allows long-term observations of single vesicles whereby inflation and deflation steps could be consecutively applied to the same vesicle. This reveals the stability of individual vesicles subjected to such osmotic changes. Figure S4a shows a GUV prepared in 66 mM glucose. GUVs are first confined in the microfluidic observation chamber as described in the previous section and the ring-valve was closed with 2 bars in the upper layer. We then partially opened the valve to allow fluid exchange with hypertonic sugar solution in the GUV exterior at a flow rate of 0.07 μl/min for about 12 minutes, after which the valve was closed. The exterior solvent is exchanged with 72 mM solvent composed of 13 wt% sucrose and rest is glucose. We observed formation of an in-necklace with 3 spherules shown in Fig. S4b. The necklace unfolds upon inflation in 66 mM glucose (Fig. S4c) and repeatedly folds again upon deflation (Fig. S4d) with the same solvent conditions. The confocal cross-sections shown in Figs. 4b,d are in the plane where the necklace can be visualized which is not the equatorial plane. We find that the overall area and volume $(A_{\rm out},\ V_{\rm out}) = (570\ \mu{\rm m}^2, 1300\ \mu{\rm m}^3)$ (in Fig. S4a) changes to $(571\ \mu{\rm m}^2, 1300\ \mu{\rm m}^3)$ (in Fig. S4b), $(600\ \mu{\rm m}^2, 1260\ \mu{\rm m}^3)$ (in Fig. S4c) and $(500\ \mu{\rm m}^2, 1000\ \mu{\rm m}^3)$ (in Fig. S4d). We provide movies (Movies S2 and S3) showing time scans of Fig. S4b and Fig. S4d to appreciate that measurement error is limited by random movement of inner buds and mother vesicle during acquisition of confocal scans.

MOVIE CAPTIONS

Movie S1. Confocal z-stacks of the GUV displayed in Fig. 2b. The GUV was prepared in 66 mM glucose and then

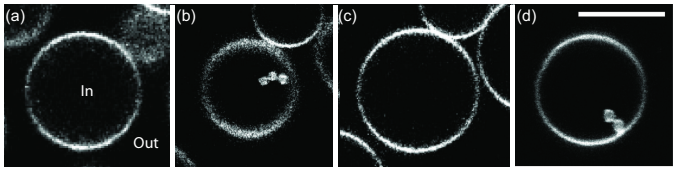

Fig. S4. Stability of GUV during multiple solvent exchange. (a) Gray scale image showing confocal cross-sections (not at the equatorial plane) of a GUV prepared in 66 mM glucose, deflated and inflated with time. (a) GUV in isotonic solution: inside and outside 66 mM glucose. (b) Same GUV undergoes deflation in 72 mM sugar solution with 13% sucrose. (c) Outside solution is exchanged with 66 mM glucose to inflate the GUV. (d) Outside solution is exchanged with 72 mM solvent same as in b and the number of in-buds is reduced to 2 from 3. The scale bar of 10 μm applies to all images.

deflated in aqueous solution of 72 mM sugar solution containing calcein (green). The movie shows contour fluctuations of outer vesicle. Presence of calcein inside the inner tube confirms osmotic deflation. The scale bar is 25 μm. GUVs membrane is composed of POPC, 10 mole% cholesterol and 0.1 mole% of membrane dye, Texas Red DHPE.

Movie S2. Confocal time-scans of the GUV displayed in Fig. S4b. Contour fluctuations and random movement for the in-necklace can be seen during the scans. The movie shows an in-necklace of three in-buds. The scale bar is 10 μm shown in the first frame.

Movie S3. Confocal time-scans of the GUV displayed in Fig. S4d. Membrane contour fluctuations for the mother GUV and necklace can be seen during the scans. The movie shows an in-necklace of two in-buds. The scale bar is 7.5 μm shown in the movie.

References

1 T. Robinson, P. Kuhn, K. Eyer and P. S. Dietrich, *Biomicrofluidics*, 2013, **7**, 044105.

2 B. Kubsch, T. Robinson, J. Steinkhler and R. Dimova, *J. Vis. Exp*, 2017, **128**, e56034.